MRI for planning and characterization of uveal melanoma patients treated with proton beam therapy

Jaarsma-Coes, M.G.

7

General discussion

This thesis is part of the Protons4Vision project which aims to improve the accuracy of proton beam therapy and ultimately save the patients vision without the need for surgergical marker placement. At the start of this thesis, ocular MRI was not yet performed regularly in a clinically setting. In the LUMC ocular MRI was mostly performed in a research setting on the ultra-high field MRI scanner. This work contributed to transitioning ocular MRI from the research setting towards the clinic without loss of image quality[1]. Through our collaboration with Philips, this protocol[2,3] is now available worldwide for all their clinical 3T scanners[4]. At the LUMC, ocular MRI is currently contributing to the diagnosis, more accurate ocular PT planning (**chapter 4**) and/or follow-up in over three patients every week.

As part of the protons4vision project, MRI scans have been used by Kilany Hassan to develop an semi-automatic segmentation pipeline to create an MRI based tumour and eye model that can be used for treatment planning[5]. The sclera, cornea, lens, vitreous body, retinal detachment and tumour can be segmented on co-registered T1- and T2-weighted images and subsequently be used to create a eye and tumour model. I used an adapted version of this segmentation technique in (**chapter 2**) to show that the eye and tumour shape does not change between scanning and treatment position.

In **chapter 3** I showed that MRI based GTV delineation has a low observer variation of 0.4mm. This uncertainty in the GTV definition is needed to determine the margin needed for MRI based ocular PT planning systems such as the dose engine developed as part of the protons4vision project[6] by Emmanuelle Fleury. This dose engine calculates the optimal gaze-angle by finding the optimal trade-off between maximizing the tumour dose and limitation of the dose to the organs at risk. Unfortunately, the normal tissue complication probability of organs-at-risk such as the retina are not yet known. This should be known before this dose engine can create clinical relevant optimal gaze-angle estimations.

7.1 Ocular MRI from a ophthalmology perspective

My work and work from and with colleges has contributed to the acceptance of MRI in ocular oncology[7]. In the second part of this discussion I would like to reflect on this work and the work of others, to highlight possible applications for ocular MRI in clinical practise.

7.1.1 Differential diagnosis

Conventional ophthalmic imaging such as ultrasound and fundoscopy is generally sufficient to differentiate UM from other intraocular masses[8,9], although in some cases not all criteria can be evaluated due to the size and/or location of the tumour or presence of opaque media such as cataract, vitreous haemorrhage or massive choroidal effusion. In these cases MRI can be used to assess different aspect of the tumour such as its origin, signal intensity and functional imaging. Although, prospective studies regarding the accuracy of MR-based differential diagnosis of intraocular masses are lacking, several studies and case reports already provide clear indications of its value for current patients[2,3,10–13].

Based on only anatomical information, such as location, origin and signal intensity from MRI, RPE adenoma's[14], neurofibroma[15] and other types of intraocular lesions[16–31] can be differentiated. However, the appearance on MRI can also be inconclusive for example in the diagnosis of leiomyoma[32,33], lymphoma[34] and differentiation between UM and intraocular metastasis[13,35]. It is therefore recommended to include functional imaging such as DWI[2,3,11,36–40] and PWI[3,41,42] to assess whether the biological characteristics match those of UM[43].

Schwannomas for example, can have similar signal intensities as (amelanotic) UM[26]. In contrast to UM, lesions can be inhomogeneous on T2 and/or show heterogeneous enhancement[17,27,35]. Moreover, in schwannomas progressive time intensity curve have been found[27] in contrast to UMs. Similarly, lymphomas can be difficult to differentiate from UM based on signal intensity alone[34], however, a lower apparent diffusion coefficient (ADC) might help to differentiate a lymphoma from UM[40].

It is important to acknowledge that not all radiological characteristics of the lesions in the differential diagnosis of UM are known, nor have a 100% specificity (figure 7.1), therefore definite diagnoses based on MRI alone can be challenging. If one or more atypical features are present in a tumour an MRI could be requested. MRI can provide detailed information on tumour localization, the layer of origin, tumour extension and perfusion[2,3] (**chapter 3,4,5,6**). In our experience this information can provide important information for the diagnosis or substantiates a (risky) biopsy especially when combined with ophthalmic imaging. However, we also found that there is a learning curve. The radiologist needs to get experience with MRI of intraocular masses and ophthalmologists need to grow in confidence in the radiologist. Having a multidisciplinary meeting discussing the MRI's can help grow understanding and confidence from both sides. Moreover, we found that providing the radiologists with a clear question on the MRI request and adding relevant clinical information is very important to help focus the assessment of the images and formulate a relevant conclusion.

For example, if there is doubt between specific diagnoses it would be helpful to provide these diagnoses options as MRI might be able to rule out one of the two.

A.

TIC shape	Progressive	Plateau	Wash-out
UM	0	14	31
Lymphoma	0	6	6
Benign	26	13	4

Peak intensity			
UM (n=42)	1.62±0.42	Ferreira	
UM (n=12)	1.53±0.29	Buerk	
Benign (n=3)	1.14±0.06	Buerk	

B.

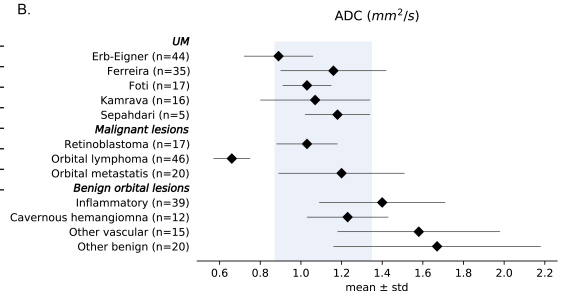

Figure 7.1: (A) UM's generally show a wash-out curve whereas most benign lesions have a progressive curve. Lesions with a plateau curve can be eighter benign or malignant. [3, 41, 42] According to Ferreira and Buerk the peak intensity of a UM is around 1.6 [3, 44]. (B) The ADC value of UM is 1.11±0.24 x10-3 mm2/s (grey area) which is lower than most benign orbital lesions and higher than orbital lymphoma. [3, 11, 37–40]

7.1.2 Therapy planning

Size is important for determination of the optimal treatment and therapy planning. For conventional radiotherapy planning of these tumours, 2D tumour dimensions are used[45]. MRI, however, provides volumetric imaging allowing tumour measurements in all possible angles, which can help to provide a better determination of the tumour prominence[2]. In general, there is an agreement between ultrasound and MRI[3]. However, for large and anterior located tumours MRI was considered more reliable **(chapter 4)**. An analysis of 72 patients, from different studies I participated in, confirmed these findings. Ultrasound measurements were slightly larger than MRI ($p<0.01$, Prominence; median 6.3mm vs 6.1mm and largest basal diameter (LBD); 14.7mm vs 14.0mm). The unreliable ultrasound measurements occurred more often in anterior tumours compared to posterior tumours (73% vs 27%, $p<0.001$), figure 7.2C. Therefore when there is doubt about tumour dimensions and small change in size could change optimal treatment or treatment is planned based on the tumour dimensions, an MRI is recommended.

The second advantage of MRI over ultrasound is that entire orbit is imaged, allowing for assessment of the relation between tumour and different organs at risk. For patients undergoing brachytherapy, MRI might be used for verification of plaque position[46,47]. MRI might also add information to the conventional model based treatment planning especially for measurements of the axial length and distance between tantalum markers and tumour in certain types of tumours

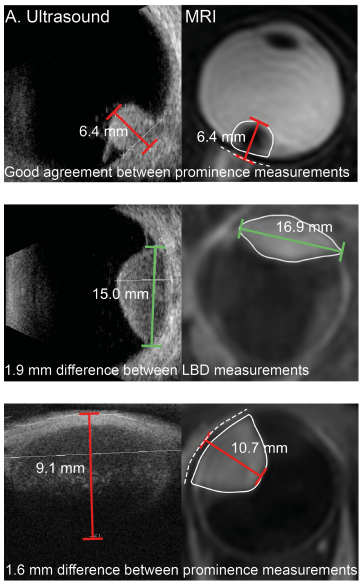

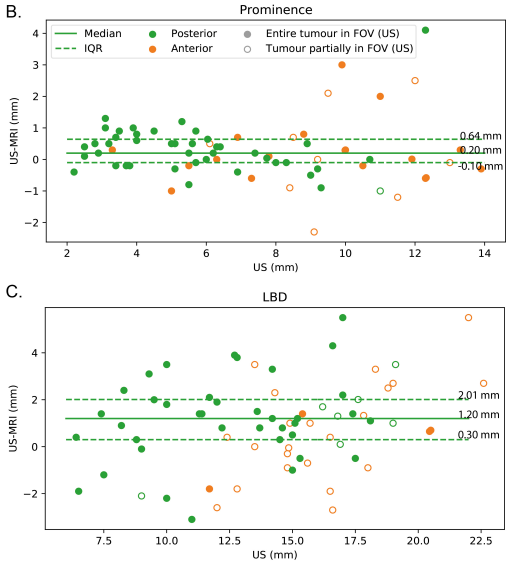

D. Absolute difference between US & MRI (mm)	median (75th percentile)	p-value
Prominence		
Posterior	0.5 (0.8)	0.31
Anterior	0.6 (1.0)	
LBD		
Posterior	1.4 (2.2)	0.20
Anterior	1.4 (2.6)	

E.	full in FOV	part in FOV	p-value (OR)	Small	Large	p-value (OR)
Prominence						
Posterior	44	1	<0.001 (0.05)	42	3	0.003 (0.12)
Anterior	18	9		17	10	
LBD						
Posterior	38	7	<0.001 (0.03)	33	12	0.13 (0.45)
Anterior	4	22		15	12	

Figure 7.2: Difference between tumour dimensions measured on US and MRI. (A) Typical examples of US and MRI measurements adopted with permission from Klaassen et al. (B,C) Difference between US and MRI with posterior tumours in green and anterior tumours in orange. The median and the inter quartile range (IQR) for the difference between MRI and US measurements is visualized for patients with an posterior tumour. (D) The prominence and LBD measurements were larger on US (Wilcoxon signed-rank test, $p<0.01$). Anterior tumours had a higher absolute difference between US and MRI for the prominence measurement. The difference in LBD is less clear. (E) Anterior tumours were more often only partially imaged. Small tumours were defined as prominence <10mm or LBD < 16mm. FOV: Field of view

(chapter 4). Moreover, it has been shown in that the inter-observer variation in the delineation of uveal melanoma is low with respect to other tumours and ultrasound **(chapter 3)**. Even though MRI based treatment planning has been investigated, it is not yet readily available in clinical practice[48–54]. On the other hand, planning systems such as OCTOPUS and RayOcular have become available and enable incorporation of MRI based information into the traditional model based treatment planning[55–58]. Importantly, it has been shown that MRI can be performed safely and reliable even with surgically placed markers and regardless of tumour and head orientation[59–61] **(chapter 2)**.

7.1.3 Follow-up

In our experience it is very important to provide patients with information about treatment response as early as possible. MRI provides the opportunity for this early treatment response monitoring especially in patients after proton beam therapy as these tumours have been shown to slowly decrease in size.

The follow-up of patients after treatment for UM is primarily focused on the reduction in tumour volume or prominence. In proton therapy however, the reduction in size, measured with ultrasound, is slow and in over 5% of the patients the tumour increases in size in the first 6-12 months[62]. Other disadvantages are the large inter-observer variation (0.3-0.6mm[63,64]) with respect to size reduction and the challenge to find the same plane as previous measurements.

Several studies showed decrease in tumour size using MRI following treatment[65–67]. Together with Michael Tang and other LUMC colleagues we compared MRI and ultrasound based measurements for proton beam therapy and brachytherapy patients. This study found that the measurements between ultrasound and MRI are comparable. Although it was found that ultrasound overestimated the tumour prominence in some patient at 3 and 6 month post treatment due to treatment related effects.

Functional imaging showed changes earlier than size and therefore allows for early treatment response monitoring[11,68]. We have shown a wash-out decrease in the majority of patients as early as 3 month after treatment (figure 1.4). It would be interesting to further quantify these changes using the method proposed in **chapter 6**. The diffusion within the tumour has shown to increase after proton beam therapy and brachytherapy[11,68,69]. Due to the large variation however, DWI might not be a useful biomarker between patients.

Finally, retinal detachment, a common complication after proton beam therapy is often treated with a vitrectomy with silicon oil tamponade. Unfortunately ultrasound imaging is hindered in these patients. Follow-up with MRI is possible

after minor adjustments in the imaging protocols **(chapter 5)**. It is important to keep in mind that for treatment response monitoring also a pre-treatment MRI is needed.

7.2 Future perspectives

With the field of ocular MRI still moving forward the possibilities and indications for ocular MRI will most likely increase. First of all, more and more patients receiving ocular PT will get an MRI. In **(chapter 4)** I showed how MRI can contribute to conventional model based ocular PT planning and we see more and more centres starting to perform MRI for this patient group. There are however prospective studies needed to evaluate the effects of MRI on the outcome in these patients. **(Chapter 3)** shows that the uncertainty in the GTV delineation is higher at the sclera edge of the tumour compared to the part of the tumour adjacent to the vitreous. In combination with known differences in uncertainties in the treatment delivery system this could be a starting point to investigate different treatment planning strategies with a margin that varies in different directions. In combination with MRI based treatment planning and the two-beam strategy proposed by Fleury et al[70] this might contribute to reduction in visual impairment after ocular PT.

In this thesis, I have addressed some challenges in the quantification of PWI. We are working together with Philips to implement $B_1{}^+$ mapping and masked registration into the DCE-MRI analysis software as recommended in **chapter 6**. Implementation of the analysis into clinical software will make quantitative functional MRI more easily available in clinical practice as it currently is a complicate and time consuming process using mostly in-house developed software. Besides implementation in the clinic, additional research in larger cohorts is needed to determine the perfusion characteristics of UM and other intraocular masses. Analysis of a large uveal melanoma cohort is needed in order to determine the expected values in uveal melanoma. It would be valuable to have similar studies to determine the anatomical and functional features of other intraocular masses to further improve the value of MRI in the differential diagnosis of intraocular masses. Moreover, a study is needed on patients with histology and a long follow-up period in order to investigate the possible prognostic value of PWI-MRI as there are already some indications that tumour perfusion can be related to monosomy 3, an important genetic marker for metastatic risk[3,39]. Finally, the first effective treatments for metastatic uveal melanoma are now becoming available[71]. These and other therapies could also be used as (neo)adjuvant treatments for high risk patients. Quantitative PWI analysis could play a role as a non invasive alternative to a biopsy in order to identify high-risk patients that

might benefit from these (neo)adjuvant treatments.

With the growing patient population and increasing cost from expensive medicines and high-tech solutions it is important to provide evidence on the cost effectiveness of ocular MRI. There are already clear indications that ocular MRI in the clinical care of uveal melanoma patients can be cost effective[72]. This should be investigated more thoroughly for different indications and health care systems.

Finally, during my thesis I experienced that the field of UM research is sometimes fragmented. One of the reasons is that treatment of UM also is fragmented. For example, it can occur that the centre for the diagnosis and the centre for treatment are over 200 km apart. I was very fortunate to be able to work in such a multidisciplinary team with people who are open for ideas and imaging techniques from other disciplines. This helped bridging the gap between disciplines and has led to new MRI sequences and protocols that improved the care for ocular oncology patients.

7.3 References

[1] M. C. Y. Tang *et al.*, "A comparison of 3 t and 7 t mri for the clinical evaluation of uveal melanoma," *J Magn Reson Imaging*, 2021, ISSN: 1053-1807. DOI: 10.1002/jmri.27939.

[2] T. A. Ferreira, L. Grech Fonk, M. G. Jaarsma-Coes, G. G. R. van Haren, M. Marinkovic, and J. M. Beenakker, "Mri of uveal melanoma," *Cancers (Basel)*, vol. 11, no. 3, 2019, ISSN: 2072-6694 (Print) 2072-6694. DOI: 10.3390/cancers11030377.

[3] T. A. Ferreira *et al.*, "Mr imaging characteristics of uveal melanoma with histopathological validation," *Neuroradiology*, 2021, ISSN: 0028-3940. DOI: 10.1007/s00234-021-02825-5.

[4] Philips. "Orbit with melanoma." (), [Online]. Available: https://www.mriclinicalcasemap.philips.com/global/case/264 (visited on 05/15/2022).

[5] M. K. Hassan *et al.*, "An automatic framework to create patient-specific eye models from 3D MR-images for treatment selection in patients with uveal melanoma," *Advances in Radiation Oncology*, p. 100 697, 2021, ISSN: 2452-1094. DOI: https://doi.org/10.1016/j.adro.2021.100697. [Online]. Available: https://www.sciencedirect.com/science/article/pii/S2452109421000555.

[6] E. Fleury *et al.*, "3D MRI-based treatment planning approach for non-invasive ocular proton therapy," *Medical Physics*, 2020, ISSN: 0094-2405.

[7] J.-W. M. Beenakker *et al.*, "Outcome measures of new technologies in uveal melanoma: Review from the european vision institute special interest focus group meeting," *Ophthalmic Research*, 2022.

[8] K. A. Roelofs *et al.*, "The moles system for planning management of melanocytic choroidal tumors: Is it safe?" *Cancers (Basel)*, vol. 12, no. 5, 2020, ISSN: 2072-6694 (Print) 2072-6694. DOI: 10.3390/cancers12051311.

[9] C. L. Shields *et al.*, "Choroidal nevus transformation into melanoma: Analysis of 2514 consecutive cases," *Arch Ophthalmol*, vol. 127, no. 8, pp. 981–7, 2009, ISSN: 0003-9950. DOI: 10.1001/archophthalmol.2009.151.

[10] P. V. Foti *et al.*, "Histopathologic and mr imaging appearance of spontaneous and radiation-induced necrosis in uveal melanomas: Initial results," *Cancers (Basel)*, vol. 14, no. 1, 2022, ISSN: 2072-6694 (Print) 2072-6694. DOI: 10.3390/cancers14010215.

[11] P. V. Foti *et al.*, "Uveal melanoma: Quantitative evaluation of diffusion-weighted mr imaging in the response assessment after proton-beam therapy, long-term follow-up," *Radiol Med*, vol. 122, no. 2, pp. 131–139, 2017, ISSN: 0033-8362. DOI: 10.1007/s11547-016-0697-3.

[12] J. W. Beenakker *et al.*, "Clinical evaluation of ultra-high-field mri for three-dimensional visualisation of tumour size in uveal melanoma patients, with direct relevance to treatment planning," *Magma*, vol. 29, no. 3, pp. 571–7, 2016, ISSN: 0968-5243 (Print) 0968-5243. DOI: 10.1007/s10334-016-0529-4. [Online]. Available: https://www.ncbi.nlm.nih.gov/pmc/articles/PMC4891368/pdf/10334_2016_Article_529.pdf.

[13] A. J. Lemke *et al.*, "Intraocular metastases: Differential diagnosis from uveal melanomas with high-resolution mri using a surface coil," *Eur Radiol*, vol. 11, no. 12, pp. 2593–601, 2001, ISSN: 0938-7994 (Print) 0938-7994. DOI: 10.1007/s003300100936.

[14] Y. Su, X. Xu, W. Wei, and J. Xian, "Using a novel mr imaging sign to differentiate retinal pigment epithelium from uveal melanoma," *Neuroradiology*, vol. 62, no. 3, pp. 347–352, 2020, ISSN: 0028-3940. DOI: 10.1007/s00234-019-02353-3.

[15] W. B. Wei, Y. Jie, J. Mo, and B. Li, "Clinical characteristics and treatment of neurofibroma of the choroid," *Chin Med J (Engl)*, vol. 125, no. 10, pp. 1832–5, 2012, ISSN: 0366-6999.

[16] E. Altun, E. Aribal, E. Toker, and M. S. Oğüt, "Anterior coloboma with macrophthalmos and cyst: Mr findings," *Clin Imaging*, vol. 29, no. 6, pp. 430–3, 2005, ISSN: 0899-7071 (Print) 0899-7071. DOI: 10.1016/j.clinimag.2005.05.001.

[17] R. C. Brennan, M. W. Wilson, S. Kaste, K. J. Helton, and M. B. McCarville, "Us and mri of pediatric ocular masses with histopathological correlation," *Pediatr Radiol*, vol. 42, no. 6, pp. 738–49, 2012, ISSN: 0301-0449 (Print) 0301-0449. DOI: 10.1007/s00247-012-2374-6. [Online]. Available: https://link.springer.com/content/pdf/10.1007/s00247-012-2374-6.pdf.

[18] P. de Graaf *et al.*, "Guidelines for imaging retinoblastoma: Imaging principles and mri standardization," *Pediatr Radiol*, vol. 42, no. 1, pp. 2–14, 2012, ISSN: 0301-0449 (Print) 0301-0449. DOI: 10.1007/s00247-011-2201-5.

[19] R. Mukhija, N. Lomi, S. Kumar, and S. Sen, "Retinoblastoma in an adult: A diagnostic dilemma," *BMJ Case Rep*, vol. 12, no. 10, 2019, ISSN: 1757-790x. DOI: 10.1136/bcr-2019-230537.

[20] L. Zhou, X. H. Zhu, K. Zhang, R. Hu, and F. Myers, "Case report: Adult retinoblastoma progression in 19 months," *Optom Vis Sci*, vol. 97, no. 11, pp. 1010–1016, 2020, ISSN: 1040-5488. DOI: 10.1097/opx.0000000000001602.

[21] R. W. Jansen *et al.*, "Mr imaging features to differentiate retinoblastoma from coats' disease and persistent fetal vasculature," *Cancers (Basel)*, vol. 12, no. 12, 2020, ISSN: 2072-6694 (Print) 2072-6694. DOI: 10.3390/cancers12123592.

[22] H. R. Garner, H. E. Fazzone, and D. E. Meltzer, "Kikuchi-fujimoto disease with bilateral uveitis," *J Radiol Case Rep*, vol. 3, no. 7, pp. 1–6, 2009, ISSN: 1943-0922 (Print) 1943-0922. DOI: 10.3941/jrcr.v3i7.188.

[23] J. C. Iturralde, C. Bianciotto, S. E. Lally, M. Krasnow, and C. L. Shields, "Massive choroidal effusion and painful secondary glaucoma from underlying uveal melanoma," *Graefes Arch Clin Exp Ophthalmol*, vol. 250, no. 4, pp. 627–30, 2012, ISSN: 0721-832x. DOI: 10.1007/s00417-011-1881-8.

[24] C. L. Shields, S. G. Honavar, J. A. Shields, J. Cater, and H. Demirci, "Circumscribed choroidal hemangioma: Clinical manifestations and factors predictive of visual outcome in 200 consecutive cases," *Ophthalmology*, vol. 108, no. 12, pp. 2237–48, 2001, ISSN: 0161-6420 (Print) 0161-6420. DOI: 10.1016/s0161-6420(01)00812-0.

[25] C. Stroszczynski *et al.*, "Choroidal hemangioma: Mr findings and differentiation from uveal melanoma," *AJNR Am J Neuroradiol*, vol. 19, no. 8, pp. 1441–7, 1998, ISSN: 0195-6108 (Print) 0195-6108.

[26] Y. J. Cho *et al.*, "A choroidal schwannoma confirmed by surgical excision," *Korean J Ophthalmol*, vol. 23, no. 1, pp. 49–52, 2009, ISSN: 1011-8942 (Print) 1011-8942. DOI: 10.3341/kjo.2009.23.1.49. [Online]. Available: https://www.ncbi.nlm.nih.gov/pmc/articles/PMC2655748/pdf/kjo-23-49.pdf.

[27] J. Xian *et al.*, "Mr imaging findings of the uveal schwannoma," *AJNR Am J Neuroradiol*, vol. 30, no. 4, pp. 769–73, 2009, ISSN: 0195-6108 (Print) 0195-6108. DOI: 10.3174/ajnr.A1467.

[28] H. Demirci, C. L. Shields, S. G. Honavar, J. A. Shields, and D. S. Bardenstein, "Long-term follow-up of giant nodular posterior scleritis simulating choroidal melanoma," *Arch Ophthalmol*, vol. 118, no. 9, pp. 1290–2, 2000, ISSN: 0003-9950 (Print) 0003-9950. DOI: 10.1001/archopht.118.9.1290.

[29] G. Kranias, C. Tyradellis, T. P. Krebs, and J. J. Augsburger, "Bilateral atypical nodular posterior scleritis," *Eur J Ophthalmol*, vol. 16, no. 4, pp. 614–7, 2006, ISSN: 1120-6721 (Print) 1120-6721. DOI: 10.1177/112067210601600419.

[30] H. Kiratli, "Persistent intraschisis hemorrhage simulating choroidal melanoma," *Jpn J Ophthalmol*, vol. 46, no. 2, pp. 222–5, 2002, ISSN: 0021-5155 (Print) 0021-5155. DOI: 10.1016/s0021-5155(01)00502-0.

[31] P. Singh, S. Sen, M. Banerjee, and R. Meel, "Choroidal melanoma masquerading as orbital cellulitis," *BMJ Case Rep*, vol. 11, no. 1, 2018, ISSN: 1757-790x. DOI: 10.1136/bcr-2018-227486.

[32] K. J. Oh *et al.*, "Mr imaging findings of uveal leiomyoma: Three cases," *AJNR Am J Neuroradiol*, vol. 26, no. 1, pp. 100–3, 2005, ISSN: 0195-6108 (Print) 0195-6108.

[33] M. N. Richter, N. E. Bechrakis, G. Stoltenburg-Didinger, and M. H. Foerster, "Transscleral resection of a ciliary body leiomyoma in a child: Case report and review of the literature," *Graefes Arch Clin Exp Ophthalmol*, vol. 241, no. 11, pp. 953–7, 2003, ISSN: 0721-832X (Print) 0721-832x. DOI: 10.1007/s00417-003-0766-x.

[34] W. Küker, U. Herrlinger, E. Grönewäller, J. M. Rohrbach, and M. Weller, "Ocular manifestation of primary nervous system lymphoma: What can be expected from imaging?" *J Neurol*, vol. 249, no. 12, pp. 1713–6, 2002, ISSN: 0340-5354 (Print) 0340-5354. DOI: 10.1007/s00415-002-0919-6.

[35] A. Mahajan, A. Crum, M. H. Johnson, and M. A. Materin, "Ocular neoplastic disease," *Semin Ultrasound CT MR*, vol. 32, no. 1, pp. 28–37, 2011, ISSN: 0887-2171 (Print) 0887-2171. DOI: 10.1053/j.sult.2010.12.001.

[36] A. R. Sepahdari, V. K. Aakalu, P. Setabutr, M. Shiehmorteza, J. H. Naheedy, and M. F. Mafee, "Indeterminate orbital masses: Restricted diffusion at mr imaging with echo-planar diffusion-weighted imaging predicts malignancy," *Radiology*, vol. 256, no. 2, pp. 554–64, 2010, ISSN: 0033-8419. DOI: 10.1148/radiol.10091956.

[37] P. de Graaf *et al.*, "Single-shot turbo spin-echo diffusion-weighted imaging for retinoblastoma: Initial experience," *AJNR Am J Neuroradiol*, vol. 33, no. 1, pp. 110–8, 2012, ISSN: 0195-6108 (Print) 0195-6108. DOI: 10.3174/ajnr.A2729.

[38] K. Erb-Eigner, G. Willerding, M. Taupitz, B. Hamm, and P. Asbach, "Diffusion-weighted imaging of ocular melanoma," *Invest Radiol*, vol. 48, no. 10, pp. 702–7, 2013, ISSN: 0020-9996. DOI: 10.1097/RLI.0b013e31828eea67.

[39] M. Kamrava *et al.*, "Quantitative multiparametric mri in uveal melanoma: Increased tumor permeability may predict monosomy 3," *Neuroradiology*, vol. 57, no. 8, pp. 833–40, 2015, ISSN: 0028-3940. DOI: 10.1007/s00234-015-1546-0.

[40] A. R. Sepahdari, L. S. Politi, V. K. Aakalu, H. J. Kim, and A. A. Razek, "Diffusion-weighted imaging of orbital masses: Multi-institutional data support a 2-adc threshold model to categorize lesions as benign, malignant, or indeterminate," *AJNR Am J Neuroradiol*, vol. 35, no. 1, pp. 170–5, 2014, ISSN: 0195-6108 (Print) 0195-6108. DOI: 10.3174/ajnr.A3619.

[41] D. J. Li *et al.*, "[comparative analysis on the significances of contrast-enhanced ultrasound and dynamic contrast-enhanced magnetic resonance imaging in uveal melanoma diagnosis]," *Zhonghua Yan Ke Za Zhi*, vol. 54, no. 3, pp. 194–198, 2018, ISSN: 0412-4081 (Print) 0412-4081. DOI: 10.3760/cma.j.issn.0412-4081.2018.03.009.

[42] Y. Yuan, X. P. Kuai, X. S. Chen, and X. F. Tao, "Assessment of dynamic contrast-enhanced magnetic resonance imaging in the differentiation of malignant from benign orbital masses," *Eur J Radiol*, vol. 82, no. 9, pp. 1506–11, 2013, ISSN: 0720-048x. DOI: 10.1016/j.ejrad.2013.03.001.

[43] M. G. Jaarsma-Coes, T. A. Ferreira, G. P. M. Luyten, and J. W. M. Beenakker, "Reaction on "ocular ultrasound versus mri in the detection of extrascleral extension in a patient with choroidal melanoma"," *BMC Ophthalmol*, vol. 19, no. 1, p. 193, 2019, ISSN: 1471-2415. DOI: 10.1186/s12886-019-1206-y.

[44] B. M. Buerk *et al.*, "Vascular perfusion of choroidal melanoma by 3.0 tesla magnetic resonance imaging," *Trans Am Ophthalmol Soc*, vol. 102, 209–15, discussion 215–7, 2004, ISSN: 0065-9533 (Print) 0065-9533.

[45] A. Kacperek, "Protontherapy of eye tumours in the UK: A review of treatment at Clatterbridge," *Applied Radiation and Isotopes*, vol. 67, no. 3, pp. 378–386, 2009, ISSN: 0969-8043. DOI: https://doi.org/10.1016/j.apradiso.2008.06.012. [Online]. Available: https://www.sciencedirect.com/science/article/pii/S0969804308003205.

[46] E. T. Detorakis *et al.*, "Mri and dual-energy ct fusion anatomic imaging in ru-106 ophthalmic brachytherapy," *Brachytherapy*, vol. 20, no. 4, pp. 828–834, 2021, ISSN: 1538-4721. DOI: 10.1016/j.brachy.2021.01.003.

[47] J. E. Zoberi *et al.*, "Mri-based treatment planning and dose delivery verification for intraocular melanoma brachytherapy," *Brachytherapy*, vol. 17, no. 1, pp. 31–39, 2018, ISSN: 1538-4721 (Print) 1538-4721. DOI: 10.1016/j.brachy.2017.07.011. [Online]. Available: https://www.ncbi.nlm.nih.gov/pmc/articles/PMC6366337/pdf/nihms-1516405.pdf.

[48] C. Ciller *et al.*, "Multi-channel mri segmentation of eye structures and tumors using patient-specific features," *PLoS One*, vol. 12, no. 3, e0173900, 2017, ISSN: 1932-6203. DOI: 10.1371/journal.pone.0173900.

[49] I. Daftari, E. Aghaian, J. M. O'Brien, W. Dillon, and T. L. Phillips, "3d mri-based tumor delineation of ocular melanoma and its comparison with conventional techniques," *Med Phys*, vol. 32, no. 11, pp. 3355–62, 2005, ISSN: 0094-2405 (Print) 0094-2405. DOI: 10.1118/1.2068927.

[50] E. Fleury *et al.*, "Three-dimensional mri-based treatment planning approach for non-invasive ocular proton therapy," *Med Phys*, vol. 48, no. 3, pp. 1315–1326, 2021, ISSN: 0094-2405 (Print) 0094-2405. DOI: 10.1002/mp.14665.

[51] S. Marnitz *et al.*, "Proton therapy of uveal melanomas: Intercomparison of mri-based and conventional treatment planning," *Strahlenther Onkol*, vol. 182, no. 7, pp. 395–9, 2006, ISSN: 0179-7158 (Print) 0179-7158. DOI: 10.1007/s00066-006-1512-1.

[52] H. G. Nguyen *et al.*, "Personalized anatomic eye model from t1-weighted volume interpolated gradient echo magnetic resonance imaging of patients with uveal melanoma," *Int J Radiat Oncol Biol Phys*, vol. 102, no. 4, pp. 813–820, 2018, ISSN: 0360-3016. DOI: 10.1016/j.ijrobp.2018.05.004.

[53] I. Seibel *et al.*, "Proton beam irradiation: A safe procedure in postequatorial extraocular extension from uveal melanoma," *Am J Ophthalmol*, vol. 191, pp. 49–53, 2018, ISSN: 0002-9394. DOI: 10.1016/j.ajo.2018.04.006.

[54] R. Via *et al.*, "Potential and pitfalls of 1.5t mri imaging for target volume definition in ocular proton therapy," *Radiother Oncol*, vol. 154, pp. 53–59, 2021, ISSN: 0167-8140. DOI: 10.1016/j.radonc.2020.08.023.

[55] B. Dobler and R. Bendl, "Precise modelling of the eye for proton therapy of intra-ocular tumours," *Phys Med Biol*, vol. 47, no. 4, pp. 593–613, 2002, ISSN: 0031-9155 (Print) 0031-9155. DOI: 10.1088/0031-9155/47/4/304.

[56] F. Hennings, A. Lomax, A. Pica, D. C. Weber, and J. Hrbacek, "Automated treatment planning system for uveal melanomas treated with proton therapy: A proof-of-concept analysis," *Int J Radiat Oncol Biol Phys*, vol. 101, no. 3, pp. 724–731, 2018, ISSN: 0360-3016. DOI: 10.1016/j.ijrobp.2018.02.008.

[57] J. Hrbacek *et al.*, "Practice patterns analysis of ocular proton therapy centers: The international optic survey," *Int J Radiat Oncol Biol Phys*, vol. 95, no. 1, pp. 336–343, 2016, ISSN: 0360-3016. DOI: 10.1016/j.ijrobp.2016.01.040.

[58] Web Page, 2020. [Online]. Available: https://www.raysearchlabs.com/media/press-releases/2020/new-release-of-groundbreaking-treatment-planning-system-raystation-provides-major-advances-for-proton-pbs-monte-carlo-with-gpu.

[59] H. M. Gach *et al.*, "Magnetic resonance imaging metal artifact reduction for eye plaque patient with dental braces," *J Contemp Brachytherapy*, vol. 9, no. 5, pp. 490–495, 2017, ISSN: 1689-832X (Print) 2081-2841. DOI: 10.5114/jcb.2017.71184.

[60] M. G. Jaarsma-Coes *et al.*, "Measuring eye deformation between planning and proton beam therapy position using magnetic resonance imaging," *Phys Imaging Radiat Oncol*, vol. 16, pp. 33–36, 2020, ISSN: 2405-6316. DOI: 10.1016/j.phro.2020.09.010.

[61] E. Oberacker *et al.*, "Magnetic resonance safety and compatibility of tantalum markers used in proton beam therapy for intraocular tumors: A 7.0 tesla study," *Magn Reson Med*, vol. 78, no. 4, pp. 1533–1546, 2017, ISSN: 0740-3194. DOI: 10.1002/mrm.26534.

[62] C. Maschi, J. Thariat, J. Herault, and J. P. Caujolle, "Tumour response in uveal melanomas treated with proton beam therapy," *Clin Oncol (R Coll Radiol)*, vol. 28, no. 3, pp. 198–203, 2016, ISSN: 0936-6555. DOI: 10.1016/j.clon.2015.08.007.

[63] D. H. Char, S. Kroll, R. D. Stone, R. Harrie, and B. Kerman, "Ultrasonographic measurement of uveal melanoma thickness: Interobserver variability," *Br J Ophthalmol*, vol. 74, no. 3, pp. 183–5, 1990, ISSN: 0007-1161 (Print) 0007-1161. DOI: 10.1136/bjo.74.3.183.

[64] C. Haritoglou, A. S. Neubauer, H. Herzum, W. R. Freeman, and A. J. Mueller, "Interobserver and intraobserver variability of measurements of uveal melanomas using standardised echography," *Br J Ophthalmol*, vol. 86, no. 12, pp. 1390–4, 2002, ISSN: 0007-1161 (Print) 0007-1161. DOI: 10.1136/bjo.86.12.1390.

[65] D. W. Kang, S. C. Lee, Y. G. Park, and J. H. Chang, "Long-term results of gamma knife surgery for uveal melanomas," *J Neurosurg*, vol. 117 Suppl, pp. 108–14, 2012, ISSN: 0022-3085. DOI: 10.3171/2012.8.Gks121002.

[66] T. W. Kim *et al.*, "Clinical outcomes of proton beam therapy for choroidal melanoma at a single institute in korea," *Cancer Res Treat*, vol. 50, no. 2, pp. 335–344, 2018, ISSN: 1598-2998 (Print) 1598-2998. DOI: 10.4143/crt.2017.070.

[67] Z. O. Toktas *et al.*, "Gamma knife stereotactic radiosurgery yields good long-term outcomes for low-volume uveal melanomas without intraocular complications," *J Clin Neurosci*, vol. 17, no. 4, pp. 441–5, 2010, ISSN: 0967-5868. DOI: 10.1016/j.jocn.2009.08.004.

[68] A. Russo *et al.*, "Diffusion-weighted magnetic resonance imaging and ultrasound evaluation of choroidal melanomas after proton-beam therapy," *Radiol Med*, vol. 120, no. 7, pp. 634–40, 2015, ISSN: 0033-8362. DOI: 10.1007/s11547-015-0509-1.

[69] F. Bitencourt *et al.*, "Response evaluation of choroidal melanoma after brachytherapy using diffusion-weighted magnetic resonance imaging (dw-mri): Preliminary findings," *Front Oncol*, vol. 10, p. 825, 2020, ISSN: 2234-943X (Print) 2234-943x. DOI: 10.3389/fonc.2020.00825. [Online]. Available: https://www.ncbi.nlm.nih.gov/pmc/articles/PMC7248391/pdf/fonc-10-00825.pdf.

[70] E. Fleury *et al.*, "Improving organs-at-risk sparing for choroidal melanoma patients: A ct-based two-beam strategy in ocular proton therapy with a dedicated eyeline," *Radiotherapy and Oncology*, 2022.

[71] Y. G. Najjar *et al.*, "Ipilimumab plus nivolumab for patients with metastatic uveal melanoma: A multicenter, retrospective study," *Journal for immunotherapy of cancer*, vol. 8, no. 1, 2020.

[72] L. G. Fonk, T. A. Ferreira, A. G. Webb, G. P. Luyten, and J. W. M. Beenakker, "The economic value of mr-imaging for uveal melanoma," *Clinical Ophthalmology*, 2020, ISSN: 11775483. DOI: 10.2147/OPTH.S238405.